HYDROLOGICAL PROCESSES
Hydrol. Process. **27**, 333–346 (2013)
Published online 19 March 2012 in Wiley Online Library
(wileyonlinelibrary.com) DOI: 10.1002/hyp.8425

Validation of a full hydrodynamic model for large-scale hydrologic modelling in the Amazon

Rodrigo C. D. Paiva,* Walter Collischonn and Diogo Costa Buarque

Instituto de Pesquisas Hidráulicas – IPH, Universidade Federal do Rio Grande do Sul – UFRGS, Av. Bento Gonçalves, 9500, Porto Alegre, 90050-260, RS, Brasil

Abstract:

A key aspect of large river basins partially neglected in large-scale hydrological models is river hydrodynamics. Large-scale hydrologic models normally simulate river hydrodynamics using simplified models that do not represent aspects such as backwater effects and flood inundation, key factors for some of the largest rivers of the world, such as the Amazon. In a previous paper, we have described a large-scale hydrodynamic approach resultant from an improvement of the MGB-IPH hydrological model. It uses full Saint Venant equations, a simple storage model for flood inundation and GIS-based algorithms to extract model parameters from digital elevation models. In the present paper, we evaluate this model in the Solimões River basin. Discharge results were validated using 18 stream gauges showing that the model is accurate. It represents the large delay and attenuation of flood waves in the Solimões basin, while simplified models, represented here by Muskingum Cunge, provide hydrographs are wrongly noisy and in advance. Validation against 35 stream gauges shows that the model is able to simulate observed water levels with accuracy, representing their amplitude of variation and timing. The model performs better in large rivers, and errors concentrate in small rivers possibly due to uncertainty in river geometry. The validation of flood extent results using remote sensing estimates also shows that the model accuracy is comparable to other flood inundation modelling studies. Results show that (i) river-floodplain water exchange and storage, and (ii) backwater effects play an important role for the Amazon River basin hydrodynamics. Copyright © 2011 John Wiley & Sons, Ltd.

KEY WORDS large-scale hydrodynamic model; Amazon; flow routing; flood inundation

Received 4 April 2011; Accepted 10 November 2011

INTRODUCTION

River hydrodynamic modelling based on Saint Venant equations is a subject that has been developed since the early 70s–80s, currently being part of the water resources engineering practice. One-dimensional hydrodynamic modelling packages are easily available, and some of them have been applied in relatively large-scale problems (Lian *et al*., 2007; Remo and Pinter, 2007; Biancamaria *et al*., 2009; Paz *et al*., 2010), but their use within large-scale distributed hydrological models, which also represent rainfall-runoff processes, is uncommon.

Large-scale hydrological models normally have specific modules for flow routing calculations. However, this type of model generally represents river hydrodynamic processes in a very simplified form. In a collection of large-scale hydrological models described by Singh and Frevert (2002), for instance, no single model had a hydrodynamic flow routing module. Most large-scale hydrological models use simplified forms of Saint Venant equations, in which the dynamic equation (or momentum conservation equation) is replaced by a simplistic relation between water volume storage within a river reach and its outflow (Vorosmarty *et al*., 1989; Liston *et al*., 1994; Coe *et al*., 2008) or by kinematic wave or Muskingum-type methods (Arora *et al*., 1999; Collischonn *et al*., 2007; Decharme *et al*., 2008; Beighley *et al*., 2009; Mauser and Bach, 2009; Dadson *et al*., 2010; Getirana *et al*., 2010; Decharme *et al*., 2011). As a consequence, important physical aspects of river hydraulics are being ignored, notably backwater effects and looped stage-discharge relations.

These issues are especially important in relatively flat river systems, like the Amazon and its tributaries, where the physical influence of sea tides can be identified more than 1000-km upstream on the main river channel (Kosuth *et al*., 2009), while the influence of the main river over its tributaries was shown by Meade *et al*. (1991). More recently, this importance was stressed by Trigg *et al*. (2009) who say that: 'Our investigations show that the Amazon flood wave is subcritical and diffusive in character and, due to shallow bed slopes, backwater conditions control significant reach lengths and are present for low and high water states'. A recent paper by Tomasella *et al*. (2010) shows that timing differences in hydrographs had a major impact on droughts of central Amazonian rivers due to backwater effects. Recently, to improve these aspects, more complex approaches have been presented where the pressure term of Saint Venant equations is introduced in a diffusion (Yamazaki *et al*., 2011) and a hydrodynamic (Paiva *et al*., 2011) based models.

*Correspondence to: Rodrigo C. D. Paiva, Instituto de Pesquisas Hidráulicas – IPH, Universidade Federal do Rio Grande do Sul – UFRGS, Av. Bento Gonçalves, 9500 - Porto Alegre, 90050–260, RS – Brasil.
E-mail: rodrigocdpaiva@gmail.com

Another important issue in large-scale hydrological modelling is the importance of floodplain inundation (Alsdorf *et al.*, 2007a; Bonnet *et al.*, 2008; Alsdorf *et al.*, 2010) and its influence on flood propagation. This fundamental aspect was recognized and included with different levels of complexity in flow routing modules of hydrological models: Beighley *et al.* (2009) estimated floodplain equivalent widths using a geomorphological equation and used it in a Muskingum Cunge model using a composed-type cross section; Yamazaki *et al.* (2011) and Paiva *et al.* (2011) consider that floodplains act as storage areas where its bathymetry is extracted from Shuttle Radar Topography Mission (SRTM) digital elevation model (DEM) (Farr *et al.*, 2007) at 30" and 15" (~1 km and 500 m), river and floodplains have same water levels, and models used 15" (~25 km) grid cell and 10-km river discretization, respectively; Decharme *et al.* (2008) and Decharme *et al.* (2011) also use a storage type model with coarse $1^{o} \times 1^{o}$ resolution (~100 km) with floodplain bathymetry estimated by the HYDRO1 K DEM at 1-km resolution, but represents the water exchange between river and floodplains as function of river-floodplain water slope and Manning's equation; Coe *et al.* (2008) used a 2D approach at 5-min resolution over the Amazon using floodplain bathymetry from 1-km resolution SRTM data set but forced results with a remote sensing based flood extent mask from Hess *et al.* (2003). However, including relatively complex modules to represent floodplain flows within large-scale models, while keeping oversimplified main channel flow routing methods, may be inadequate, as suggested by Trigg *et al.* (2009), who emphasize that 'it is important to get the hydraulics of the main channel right before tackling the more complex interactions with the floodplain'.

All large-scale flow routing methods require geometric information, such as river lengths, width and floodplain geometry, where part is estimated based on DEMs and part is treated as parameters. However, many of the simplified flow routing models also use calibration parameters to compensate the lack of physical representation, and these have to be calibrated or tuned using observed discharge data. Flow routing methods based on full Saint Venant equations have a single parameter (Manning's n), for which a relatively narrow range of values is known from previous applications of such models and from published tables, as in Chow (1959). Therefore, the later should be preferred due to its expected higher predictive capability outside the observed data range, such as extreme events and scenarios of land use and climate change.

Saint Venant equations are solved for two variables at each computational cross section: discharge (or velocity) and water level height. Simplified models, on the other hand, generally provide only discharge results, from which water level height may be derived by further assumptions (e.g. normal flow, rating curves, water slope parallel to bed slope). Independent results of water level height are highly desirable by several reasons: the knowledge of water levels is more important than discharge for several applications such as flooding alerts and navigation; water levels are increasingly being measured at a multitude of points thanks to remote sensing (Frappart *et al.*, 2006; Alsdorf *et al.*, 2007b; Durand *et al.*, 2010). Results of flow routing methods based on full Saint Venant equations can be directly compared with water levels measured by remote sensing, and in the future, these water levels may be useful for data assimilation into the hydrological models, reducing their uncertainty in applications such as real-time forecasts.

Finally, some of the simplified flow routing models have been shown to be non-conservative, presenting volume conservation errors exceeding 10% (Tang *et al.*, 1999; Perumal and Sahoo, 2008). This problem may be solved by changing the numerical scheme, as proposed by Todini (2007), but it is usually absent when full Saint Venant equations with traditional numerical methods are used.

In a previous paper (Paiva *et al.*, 2011), we have described the introduction of a full hydrodynamic module for flow routing within the MGB-IPH large-scale hydrological model (Collischonn *et al.*, 2007a). It is a full physical-based model that simulates discharge, water level and flood inundation, being prepared for large-scale applications using GIS-based algorithms for parameter extraction from DEMs. In the present paper, we describe the validation of this model in the Solimões/Amazon River basin. The first goal is to validate model discharge results against observations and compare this new methodology with simplified flow routing algorithms represented by the previous version of MGB-IPH. We also evaluate the accuracy of water levels and flood extent. Then, we investigate what physical processes have major influence on the differences between the stream flow model results.

THE HYDROLOGICAL-HYDRODYNAMIC MODEL

The MGB-IPH model is described in Collischonn *et al.* (2007) and Allasia *et al.* (2006). It is a large-scale distributed hydrological model that uses physical and conceptual equations to simulate land surface hydrological processes. It uses a catchment-based discretization and the hydrological response units (HRUs) approach. The simulated vertical hydrological processes include soil water budget using a bucket model, energy budget and evapotranspiration, interception, soil infiltration and run-off computed based on the variable contributing area concept and also subsuperficial and groundwater flow generation. The flow generated within the HRUs of each catchment is routed to the stream network using three linear reservoirs representing the baseflow, subsurface flow and surface flow. In the original version of the MGB-IPH, streamflow is routed through the entire river network using the Muskingum-Cunge (MC) method. Further details of the MGB-IPH model characteristics can be found in Collischonn *et al.* (2007), while some of the model applications are presented by Collischonn *et al.* (2005), Collischonn *et al.* (2008) and Getirana *et al.* (2010).

A new flow routing algorithm for MGB-IPH was developed by Paiva *et al.* (2011). It is a limited data and GIS based large-scale hydrodynamic modelling approach, and it differs from the previous one by its capability of

simulating flood inundation and backwater effects. The model solves the full 1 D Saint Venant equations (Cunge *et al*., 1980) for a river network with multiple confluences using an implicit finite difference numerical scheme similar to the Preissman scheme (Cunge *et al*., 1980) and Gauss elimination procedure based on a skyline storage method developed by Tucci (1978) and modified by Paiva *et al*. (2011).

River reaches are discretized into sub-reaches, and the hydraulic variables are computed at cross sections located at both ends of the sub-reaches. The model also divides the catchments into 'floodplain units', which are the contributing areas to each sub-reach and are used for flood inundation computations.

The flood inundation is simulated using a simple storage model (Cunge *et al*., 1980), which assumes that (i) the flow velocity parallel to the river direction is null on the floodplain, (ii) the floodplains units act only as storage areas, (iii) the floodplain water level equals the water level at the main channel and (iv) the floodplain lateral exchange equals $q_{fl} = (dz/dt)Afl(z)/dx$ where x and t are spatial and time dimensions and z is the river water level, and $Afl(z)$ is the flooded area inside a floodplain unit.

The computational river network and its parameters are defined using automated procedures based on a DEM and GIS algorithms (Paiva *et al*., 2011). River cross-section geometry is approximated by a rectangular shape with parameters width B and maximum water depth H estimated using geomorphologic equations (presented in section 3.3). River bottom level is estimated from the DEM considering corrections to avoid errors due to vegetation and water level effects. The algorithm delineates discrete 'floodplain units' for each sub-reach and extracts a z *versus* Afl curve from the DEM corrected to avoid errors due to vegetation. The model also generates flood inundation results in terms of 2 D water levels by a combination of 1 D hydrodynamic water level outputs, the floodplain unit map and the DEM.

METHODS

The Solimões river basin

Solimões River is the main tributary of Amazon River (Figure 1), and its drainage area equals 2.221.990 km^2, i.e. 36% of the whole Amazon River basin. The basin has most of its area in the Brazilian territory, but it also covers large areas of Peru, Colombia and Ecuador. Land cover is dominated by the rain forest. Solimões River drains a large area of Peru, and lots of its tributaries come from the Andean region. In the Brazilian part of the basin, relief is relatively flat, and wide floodplains are found along the main rivers. The main Solimões River tributaries in Brazil are Japurá River from the left margin and Juruá and Purus Rivers from the right.

The Solimões River basin was chosen because fluvial hydraulics is the major control of the hydrological processes. Flood wave travel time along Solimões River and its tributaries is very long, being of the order of a couple of months, as it can be seen in Paiva *et al*. (2011) for Purus River. Large seasonally flooded areas are also observed (Sippel *et al*., 1998; Hess *et al*., 2003), and important backwater effects are present, as reported by Meade *et al*. (1991) in Purus River.

Data

We used a 15" resolution DEM15s from Hydrosheds (Lehner *et al*., 2006), which is based on the SRTM (Farr *et al*., 2007). We also used the vector river network map

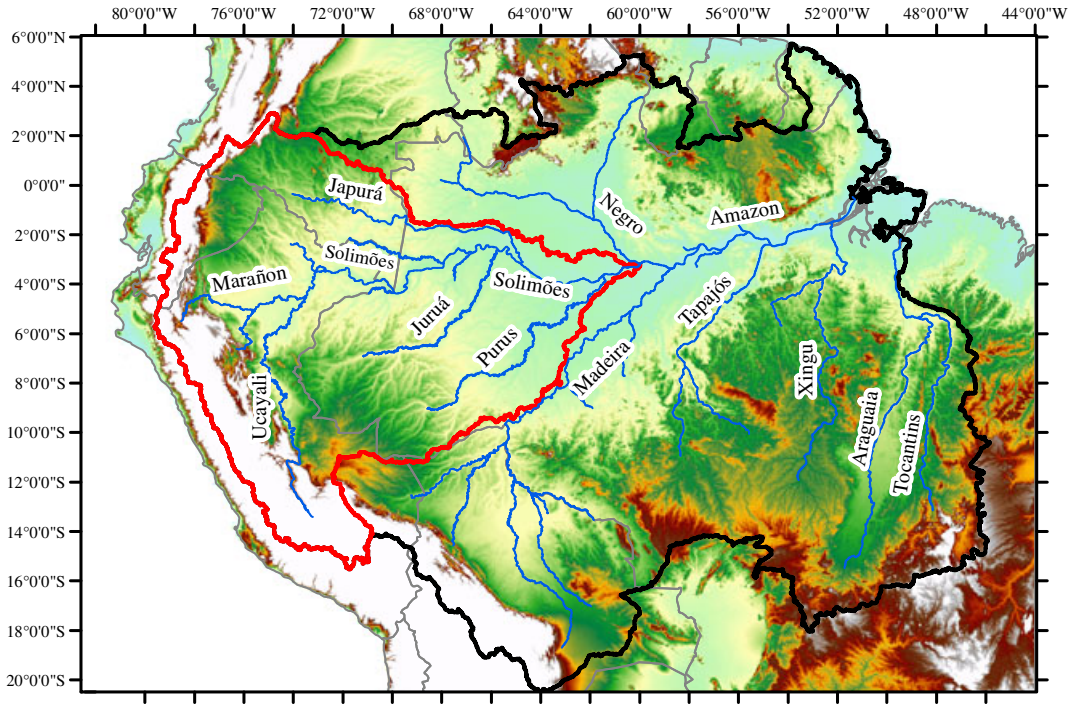

Figure 1. Solimões River basin inside the Amazon

provided by Agência Nacional de Águas (ANA) (ANA, 2006) to force the DEM using the AgreeDEM algorithm (Hellweger, 1997) for using it in flow direction computations (Paiva *et al*., 2011). A HRU map with five classes was developed combining the 'Vegetation Map of South America' (Eva *et al*., 2002) and a soil map based on RADAMBRASIL(1982) and SOTERLAC/ISRIC (Dijkshoorn *et al*., 2005) for areas outside Brazil. The National Centers for Environmental Prediction/National Center for Atmospheric Research (NCEP/NCAR) reanalysis (Kalnay *et al*., 1996) was used as the model meteorological forcing. We used daily precipitation data from rain gauges provided by ANA, but NCEP reanalysis on rainfall data was used in areas outside Brazil because rain gauge data are very scarce in such regions. The model was validated using daily discharge and water level data from 32 and 35 stream gauges, respectively (Figure 2). Flood extent results were also compared with the dual-season mapping of wetland inundation developed by Hess *et al*. (2003) using JERS-1 SAR data for two time period - 1996 high water and 1995 low water periods.

Model construction

The model discretization into river reaches, catchments, hydrodynamic computational cross sections and parameter estimation was done using the DEM and GIS-based algorithms described in Paiva *et al*. (2011). The Solimões river basin was divided into 2083 river reaches and catchments, with a mean drainage area of 1066 km^2. Model simulations were limited mostly to the Brazilian part of the Solimões river basin due to scarce gauge precipitation data outside Brazil and also some uncertainty about reanalysis or remote sensing rainfall estimates. Considering the objectives of this paper, it should be better to simulate a smaller area than to have uncertainty in the results due to large precipitation errors. Therefore, observed discharge data from gauges 1 (11400000) and 18 (12845000) were used as a boundary condition for Solimões and Japurá rivers at the border of Brazil with Peru and Colombia, respectively (Figure 2). These two rivers drain most of the area of the basin that is outside Brazil. Since there is no discharge data available in the other rivers crossing the Brazilian border, there are still small areas outside Brazil that are simulated using rainfall from the NCEP reanalysis. We also used observed water level as a downstream boundary condition in the confluence of Solimões and Negro Rivers.

In high slope reaches, the flood waves can be approximated by a kinematic wave. In order to avoid high computational efforts, some of the reaches were not simulated with the hydrodynamic model (HD), the MC model being used instead. River reaches simulated with the HD model were selected using the following criteria, as described in Paiva (2009): (i) slope lower than 20 cm/km, based on Ponce (1989) criteria for applicability of kinematic wave models; (ii) presence of large floodplains using DEM inspection; (iii) river reaches downstream to the two boundary conditions on the Brazilian border; (iv) continuity of the HD river network. As a result, 40% of the catchments were simulated using the HD model.

River reaches were then discretized considering the distance between two computational cross sections $\Delta x =$ 10 km, based on the criteria of the HD numerical scheme performance (Cunge *et al*., 1980; Castellarin *et al*., 2009; Paiva *et al*., 2011). The resulting simulated system is composed by 432 river reaches, 2492 computational cross sections, 195 confluences and 196 upstream boundary conditions. Temporal discretization for both HD and MC models is $\Delta t = 3600$ s, based on Courant criteria.

Geometric parameters of the computational cross sections, i.e. river width B [m] and maximum water depth H [m], were estimated as a function of the drainage

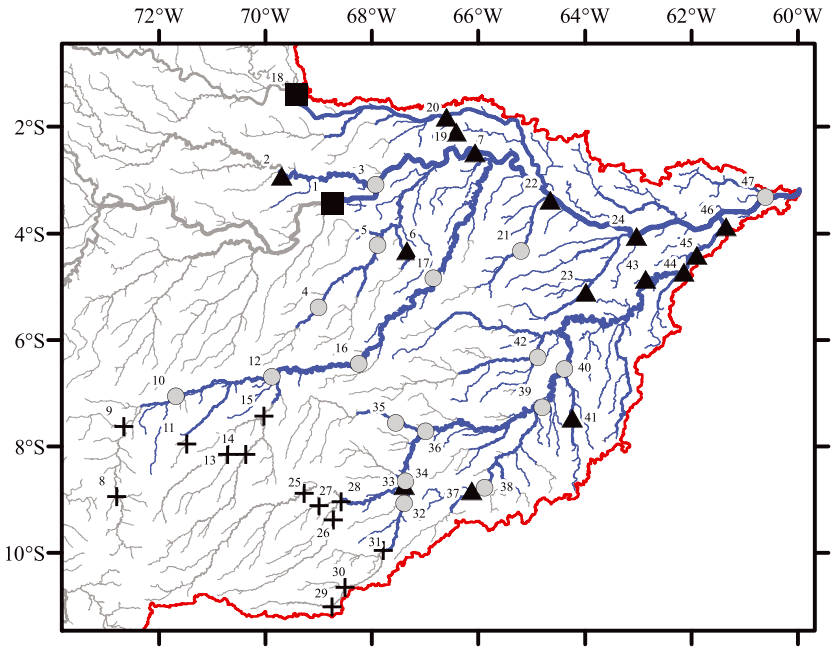

Figure 2. Stream gauge stations used for model validation using discharge data (black crosses), water level data (black triangles) and both (grey circles) data. The two black rectangles are the stream gauges used for discharge boundary conditions of the model at the Brazilian border (see section 3.3)

area Ad [km^2], using the following geomorphologic equations: $B = 0.8054Ad^{0.5289}$ and $H = 1.4351Ad^{0.1901}$ (Paiva *et al.*, 2011). Only for Solimões River we used a river width based on satellite image and equal to 3 km.

The MGB-IPH model parameters were calibrated against discharge data using the MOCOM-UA optimization algorithm (Yapo *et al.*, 1998) and the following approach. Model runs used the MC model for flow routing to avoid high computational effort. The average of the statistics E_{NS}, E_{NSlog} and ΔV (described in the next section) from streamflow stations, considering the 1986 to 2005 period, were used as objective functions. We also used only 13 stations located on the upper part of Purus and Juruá Rivers, where river reaches were not selected for hydrodynamic modelling (Figure 3). We calibrated four parameters in each of the five model HRUs, and also three parameters related to surface, subsurface and base flow within the catchments, giving rise to a total of 23 parameters. Then, these parameters were used in the whole Solimões River basin, and model results were validated using downstream streamflow gauges. Note that the parameters related to the MC and HD models were not calibrated, and we used Manning coefficient $n = 0.030$, mean effective vegetation height to correct the DEM $Hveg = 17$ m, and parameters related to river bottom level estimation $it_{max} = 5000$, $\alpha = 0.8$, $\beta = 1.0$ (Paiva *et al.*, 2011). Calibration was performed only against discharge data of the upper part of the Purus and Jurua river basins (Figure 3). Discharge data from other gauges, water level data and flood extend data were used only in model validation.

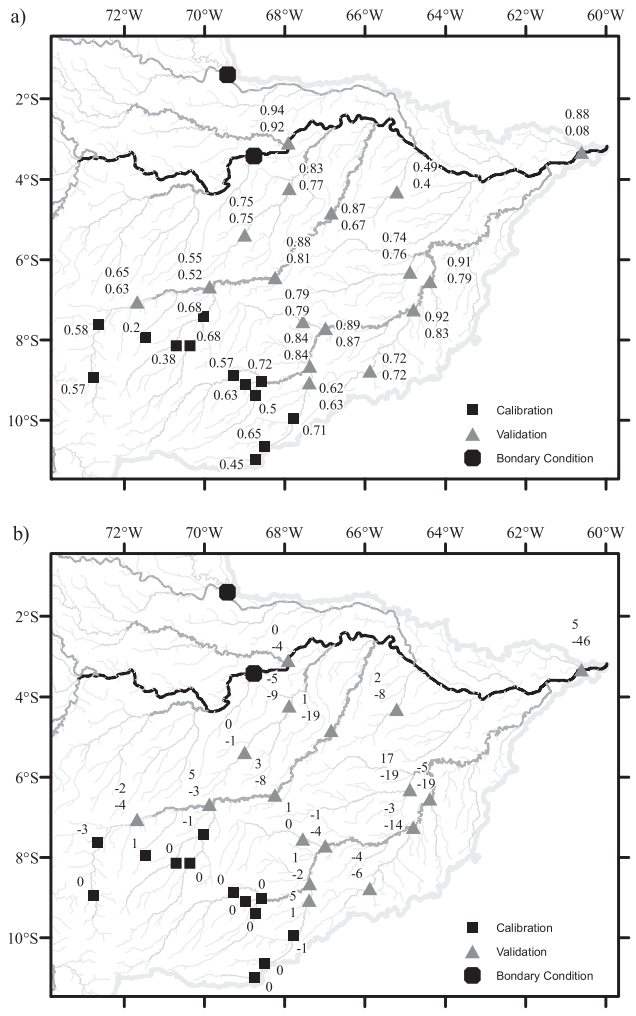

Figure 3. Nash and Sutcliffe index (a) and delay index (b) for discharges on stream gauge stations. Calibration gauges are drawn in black rectangles, validation gauges in grey triangles and discharge boundary conditions in black circles. Upper (lower) values are from HD (MC) model runs

Model performance statistics

River discharge results were compared with observations using some statistics commonly used in hydrological modelling studies: (i) Nash–Suttcliffe coefficient E_{NS} (Nash and Sutcliffe, 1970); (ii) log-Nash–Suttcliffe coefficient E_{NSlog} (Collischonn *et al.*, 2007), i.e. E_{NS} computed using a logarithm transformation on discharge time series to focus on low flows; (iii) and relative bias ΔV [%]. We also used an index to measure errors related to time delay between simulated and observed hydrographs. We call it 'delay index' *DI* [days], and it is computed using the cross correlation function $R_{xy}(m)$ from simulated (x) and observed (y) discharge time series. The *DI* equals the value of the time lag m where $R_{xy}(m)$ is maximum.

Water level results were not directly compared with observations since observed water level data are based on an arbitrary datum. The following correction was used for both observed and simulated water levels to keep these in the same reference: $y_t = z_t - \bar{z}$, where y_t is the corrected water level, z is the original water level, $\bar{z}$ is the average value of the z time series and t denotes the time interval. Then, the corrected observed and simulated water levels were compared using E_{NS}, *DI* and the correlation coefficient *R*. We also measured the water level amplitude error *A*'. Water level amplitude *A* is defined here as the difference between the 95% and 5% water level percentiles, and the amplitude error is defined as $A' = 100.(A_{calc}\text{-}A_{obs})/A_{obs}$, where A_{calc} and A_{obs} are the simulated and observed water level amplitudes.

Simulated flooded area extent in a given time interval were compared with observations using the following classical skill scores for forecast verification of discrete variables (Wilks, 2006): the threat score (*TS)* to measure the model accuracy (equal to the index used to test flood inundation models by Horritt and Bates, 2002; and Horritt and Bates, 2001, the bias index (*BIAS)*, the false alarm ratio (*FAR)* to measure the fraction of simulated flooded areas that are incorrect and the missed flooded areas ratio (*MFR)* to measure the fraction of observed flooded areas that are not predicted by the model. Those scores are determined using the following relations

$$TS = \frac{a}{a+b+c}, BIAS = \frac{a+b}{a+c}, \qquad (1)$$

$$FAR = \frac{b}{a+b}, MFR = \frac{c}{a+c}$$

where a is the total flooded area that is both observed and predicted, b is the predicted but not observed flooded

area, *c* is the observed but not predicted flooded area and *d* is the nonflooded area that is both observed and predicted.

RESULTS AND DISCUSSION

Hydrodynamic versus Muskingum-Cunge

In this section, we evaluate if the large-scale hydrodynamic modelling approach developed in Paiva *et al.* (2011) is able to provide accurate streamflow results and if it is better than simplified flow routing algorithms. We compare the results of two model runs, one using the MC model and the other the HD.

First, we show in Table I results from the calibration of the MGB-IPH model parameters. Mean values of E_{NS}, E_{NSlog}, ΔV and DI are 0.56, 0.62, 13% and −0.5 days, respectively. Model performance is worst in the uppermost part of Purus and Juruá Rivers (Figure 3). However, the errors are smaller at the downstream gauges, e.g. the average E_{NS} of the four lower gauges equals 0.67. The DI index is very low for all gauges. Model performance in calibration is comparable to other modelling studies in the Amazon region using MGB-IPH (e.g. Collischonn *et al.*, 2008) and can be considered sufficient for the objectives of this study.

Validation results were first evaluated in Purus and Juruá Rivers. Hydrographs in upper Purus and Juruá Rivers are noisy and not regularized, and, as flood waves travel downstream, they get very attenuated and delayed, and hydrographs are smoother (Figure 4). That is probably due to water storage into floodplains, which is in accordance to Wong and Laurenson (1983), who report the reduction on flood wave celerity due to river overflow.

Results of both model runs are similar in the upstream part of Juruá and Purus Rivers (Figures 3 and 4). The E_{NS} index for the HD/MC runs equals 0.65/0.63 and 0.85/0.85 in gauges 10 (12520000) and 34 (13710001), the uppermost of Juruá and Purus Rivers, respectively, while DI indexes are low and equal −2/-4 and 1/-2 days. That is possibly because the overland flow propagation within catchments dominates hydrographs characteristics. However, as the flood wave travels downstream, MC results deviate from observations, and the differences between HD and MC runs are accentuated (Figures 3 and 4). The HD model is capable to simulate the flood wave attenuation and delay, while MC hydrographs are wrongly noisy and in advance. In the most downstream gauges of Juruá and Purus (17/12840000 and 40/13880000), E_{NS} equals 0.87 and 0.91 in the HD run, respectively, and in MC run, it decreases to 0.67 and 0.79. Flood waves simulated by MC model at the same gauges are also 19 days in advance, which is a large delay if compared with the flood wave travel time (~ 1 to 2 mouths), while DI indexes are low on the HD model run (1 and −5 days).

Table I. Model performance statistics for discharge on the stream gauges used for model calibration

ID	Gauge code	River	E_{NS}	E_{NSlog}	ΔV(%)	DI(dias)
8	12370000	Juruá	0.57	0.60	17.4	0
9	12500000	Juruá	0.58	0.57	24.2	−3
11	12530000	Gregório	0.20	0.22	29.5	1
13	12600001	Tarauacá	0.38	0.67	29.6	0
14	12650000	Envira	0.68	0.74	2.8	0
15	12680000	Tarauacá	0.68	0.78	18.9	−1
25	13180000	Purus	0.57	0.65	−1.5	0
26	13300000	Iaco	0.50	0.68	−15.6	0
27	13405000	Caeté	0.63	0.39	2.9	0
28	13410000	Purus	0.72	0.77	8.8	0
29	13470000	Acre	0.45	0.61	2.9	0
30	13550000	Acre	0.65	0.70	8.8	0
31	13600002	Acre	0.71	0.68	5.1	−1

The Solimões River hydrograph has expressive regularization in the border between Brazil and Peru, and the flood wave takes 1 or 2 months to reach its confluence with Negro River, close to the Manacapuru gauge station (gauge 47/14100000). The hydrograph in this gauge (Figure 4) reveals that the performance of the HD model is excellent in Solimões River: the E_{NS} and E_{NSlog} indexes are high, both equal to 0.88; the DI index is 5 days, i.e. insignificant if compared to the flood wave travel time of Solimões River; the bias is small ($\Delta V = -4.1\%$). In contrast, errors in MC model results are very large (Figure 4): the flood wave is very advanced ($DI = -46$ days); the E_{NS} and E_{NSlog} equal 0.08 and −0.04, pointing to a very poor MC model performance.

Table II presents the model performance statistics of the MC and HD model runs for each stream gauge station. Mean values of E_{NS}, E_{NSlog}, ΔV and DI for the HD model are 0.78, 0.77, 9.7 % and 3.5 days, respectively, pointing to good model performance (similar to other modelling studies in the Amazon such as Collischonn *et al.*, 2009). Differences between both models are pronounced, and the model performance of the MC model is worse ($E_{NS} = 0.69$, $E_{NSlog} = 0.71$, $DI = 9.8$ days). Table II shows that the HD model performed better in terms of E_{NS}, E_{NSlog}, and DI indexes in 11, 11 and 14 gauges, respectively, while the MC model in only 2, 2, and 3 gauges.

Validation of water level results

In this section, we evaluate if the large-scale hydrodynamic modelling approach is able to simulate water levels with accuracy. Results from the HD run were compared with observed water levels from 35 stream gauge stations (e.g. Figure 5). These are grouped according to their location: (1) small tributaries of Solimões River; (2) tributaries of Purus River and Japurá River; (3) main Solimões tributaries, namely Purus, Juruá and Jutaí; and (4) Solimões River. We verified the overall model accuracy (E_{NS} index) and investigated if the model is able to reproduce the amplitude of variation of water levels (A' index) and the timing of flood waves (DI index).

The best model accuracy occurs in Solimões River (see Figure 6). The R and E_{NS} indexes are elevated on its six validation sites (mean values are $R = 0.98$ and $E_{NS} = 0.95$). Mean values of A' and DI are low ($A' = 10\%$ and $DI = 3$ days) and show that the model is accurate to represent the water level amplitude ($A_{obs} = 10.4$ m) and timing (Figure 5, gauge 7). Model results were also accurate in the main tributaries of Solimões River (group 3), as

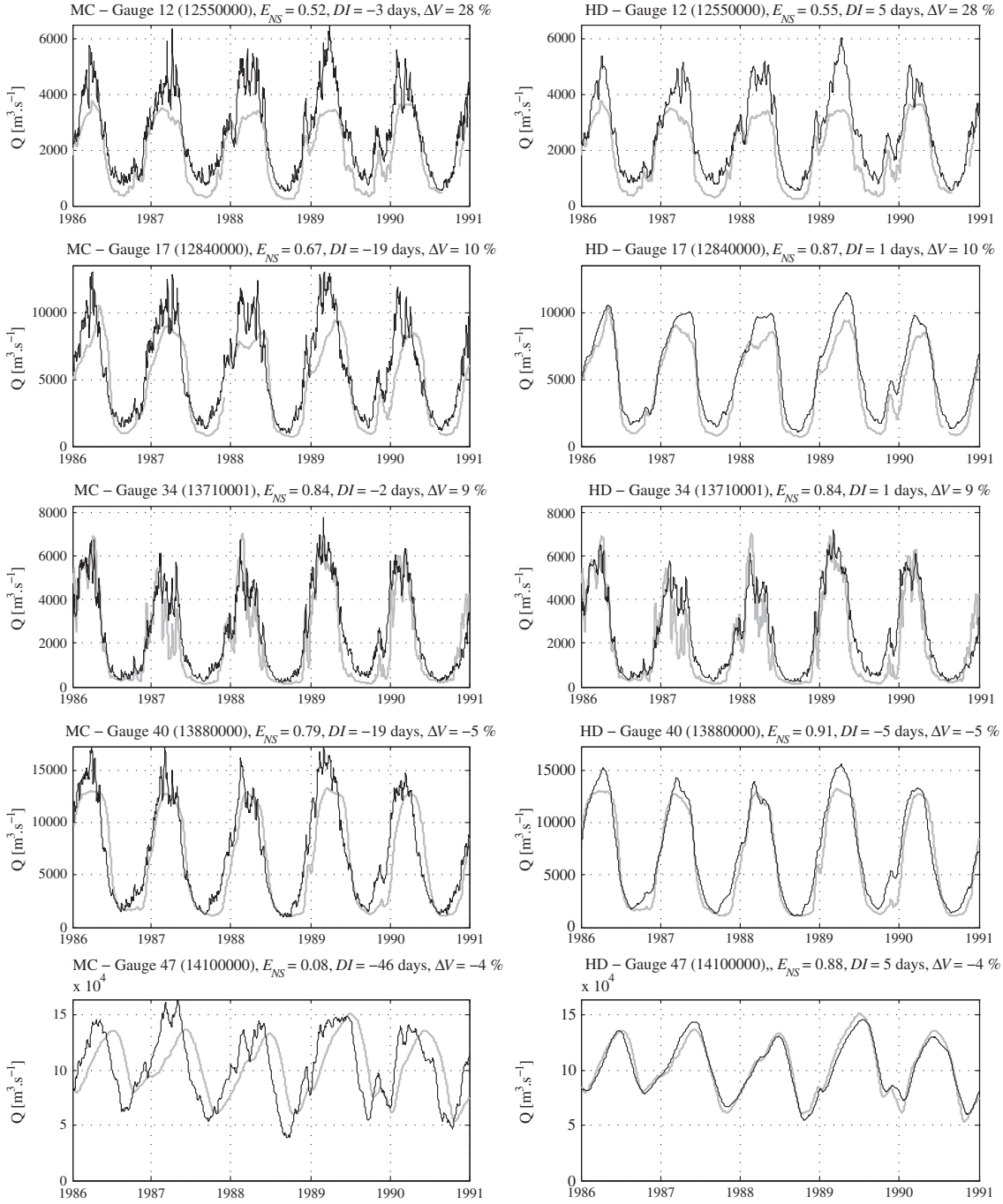

Figure 4. Observed (grey line) and simulated (black line) daily discharges in five stream gauges of the Solimões River Basin in the 1986 to 1991 time period. Figures from the left (right) present results from the MC (HD) runs

illustrated in Purus River (Figure 5, gauge 45). Mean model performance statistics were $R = 0.94$, $E_{NS} = 0.83$, $A' = 19\%$ and $DI = 4$ days.

Table III shows that in terms of overall model accuracy (E_{NS} index), large errors are concentrated in small rivers (groups 1 and 2). Errors may be due to uncertainty in meteorological forcing, in accordance with Nijssen and Lettenmaier (2004) that showed for a large-scale hydrological model that errors in precipitation cause larger errors in simulated stream flow in small drainage areas, and these errors decreased as basin area increases. However, the following discussion shows that errors in river geometry play an important role. Small tributaries of Solimões River (group 1) present the largest values of DI index ($DI = 42$ days) and smaller correlation coefficient ($R = 0.61$), indicating that the error in timing causes small E_{NS} values ($E_{NS} = 0.05$), as illustrated in Figure 5, gauge 23. These rivers are located in the central Amazon plain, and their water levels are possibly controlled by both upstream flow and Solimões backwater effects. Errors in river bottom level estimates could give rise to errors in the extension of backwater effects and in the timing of flood waves. In contrast, gauges located in smaller Purus river tributaries present small DI values ($DI = 5$ days) but concentrate the largest errors in amplitude ($A' = 67$ %), giving rise to small E_{NS} values ($E_{NS} = 0.40$). In these

Table II. Model performance statistics for discharge on the stream gauges used for model validation

			E_{NS}		E_{NSlog}		DI(days)		ΔV(%)
ID	Gauge code	River	MC	HD	MC	HD	MC	HD	-
32	13650000	Acre	**0.63**	0.62	0.75	0.75	**1**	5	−12.1
38	13849000	Ituxi	0.72	0.72	0.75	**0.76**	−6	**−4**	−24.0
10	12520000	Juruá	0.63	**0.65**	0.57	0.57	−4	**−2**	24.4
12	12550000	Juruá	0.52	**0.55**	0.65	**0.66**	**−3**	5	28.0
16	12700000	Juruá	0.81	**0.88**	0.79	**0.82**	−8	**3**	3.4
17	12840000	Juruá	0.67	**0.87**	0.77	**0.84**	−19	**1**	9.6
4	12100000	Jutaí	0.75	0.75	0.67	0.67	−1	**0**	1.7
5	12200000	Jutaí	0.77	**0.83**	0.81	**0.85**	−9	**−5**	−0.1
42	13886000	Mucuim	**0.76**	0.74	**0.78**	0.75	−19	**17**	−3.4
35	13740000	Pauini	0.79	0.79	0.72	0.72	**0**	1	1.8
34	13710001	Purus	0.84	0.84	0.78	**0.79**	−2	**1**	9.0
36	13750000	Purus	0.87	**0.89**	0.87	**0.89**	−4	**−1**	−0.9
39	13870000	Purus	0.83	**0.92**	0.84	**0.90**	−14	**−3**	5.1
40	13880000	Purus	0.79	**0.91**	0.82	**0.91**	−19	**−5**	−4.7
3	11500000	Solimões	0.92	**0.94**	0.91	**0.93**	−4	**0**	−6.1
47	14100000	Solimões	0.08	**0.88**	−0.04	**0.88**	−46	**5**	−4.1
21	12880000	Tefé	0.40	**0.49**	**0.57**	0.45	−8	**2**	26.4
	Mean		0.69	**0.78**	0.71	**0.77**	9.8	**3.5**	9.7
	90%		0.85	**0.91**	0.85	**0.90**	19.0	**5**	25.2
	50%		0.76	**0.83**	0.77	**0.79**	6.0	**3**	5.1
	10%		0.47	**0.59**	0.57	**0.62**	1.0	**0**	1.4
	N[b]		2	**11**	2	**11**	3	**14**	-

[a] Statistics computed from absolute values for the indexes DI and ΔV.
[b] Number of gauges where the respective model performed better than the other.
[c] Bold values indicate better model performance when comparing MC and HD model runs for each gauge and each index.

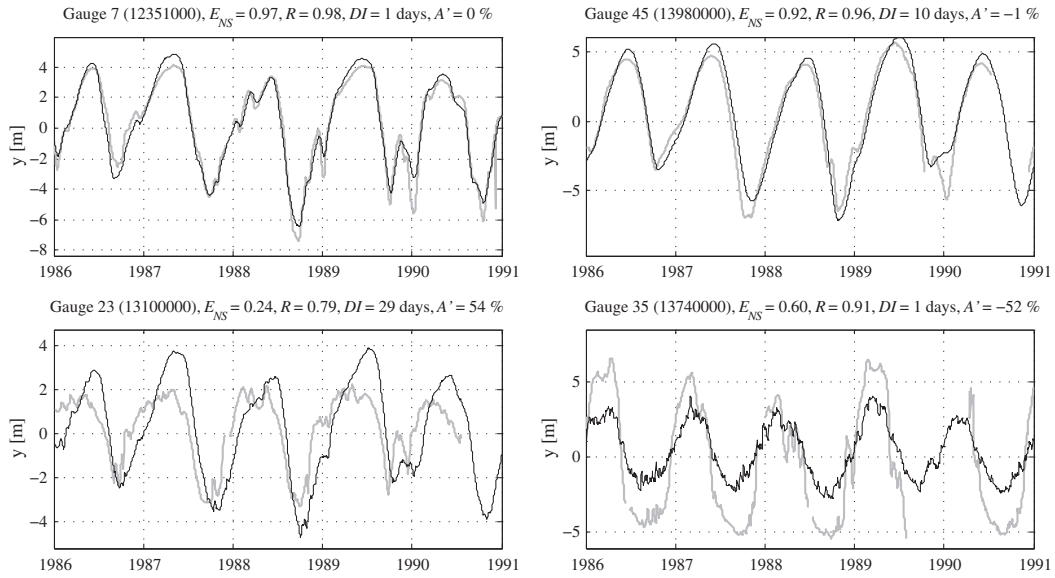

Figure 5. Observed (grey line) and simulated (black line) daily water levels in four stream gauges of the Solimões River basin in the 1986 to 1991 time period

rivers, water levels are controlled mainly by upstream flow and river cross-section geometry. In many cases, discharge may be well represented even with errors in water levels due to uncertainty in cross-section geometry. This can be seen by the results that show for these sites observed and simulated water levels highly correlated ($R = 0.93$) but large amplitude errors (Figure 5, gauge 35), which indicates that model errors are due to the uncertainty of the cross-section geometry (e.g. river width).

Model performance is good in larger rivers, and the uncertainty observed in smaller rivers results from errors in river geometry. However, the overall model performance can be considered good, since in 50% of the validation sites, $R > 0.94$, $ENS > 0.81$, $A' < 23\%$ and $DI < 4$ days.

Validation of flooded area results

Simulated flood extent was validated against remote sensing estimates from Hess *et al.* (2003) (Figures 7b and 8b).

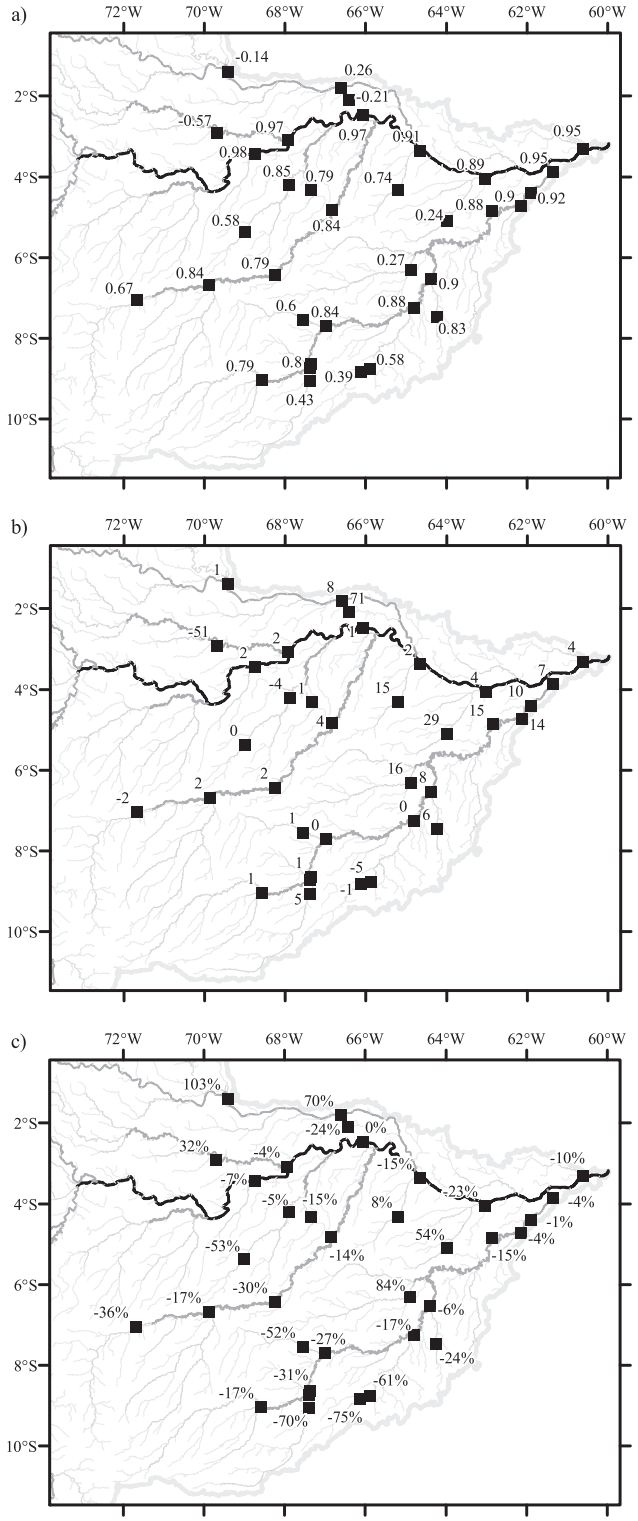

Figure 6. Nash and Sutcliffe index E_{NS} (a), delay index *DI* (b) and amplitude error *A*' (c) for water levels on stream gauge stations

We considered it as the 'true' flood extend and computed model errors by comparing it with the simulated flood extent for Oct15-1995 and May15-1996 (Figures 7a and 8a). Model flood inundation and comparisons were computed in a 15" (~500 m) resolution grid. We also present an error map showing areas were correctly predicted flooded or nonflooded areas of the model and also flooded areas predicted as nonflooded or nonflood areas predicted as flooded.

The model was able to represent the high water flood extent (Figure 7), showing agreement with observations in the floodplains of Solimões, Purus, Japurá and other major tributaries: simulated flood extent is 19% lower than the observed one; *TS* is larger ($TS = 0.70$) than presented in other flood modelling studies (Horritt and Bates, 2001; Horritt and Bates, 2002); and false alarm ratio is low ($FAR = 0.08$). Most errors are found in the upstream Jutaí and Juruá Rivers, where the model did not predict the observed inundation. Actually, *MFR* indicates that 26% of the observed flooded areas are not predicted.

Model performance is worse in low water periods, as indicated by a lower *TS* index ($TS = 0.34$) and Figure 8. The model correctly predicts flooded areas inside large rivers. However, there are permanent flooded areas (marginal lakes) in Purus and Juruá floodplains that are not predicted, and consequently the *MFR* index is elevated ($MFR = 0.42$). There are also errors in floodplains of Solimões and Japurá Rivers, where flood extent is overestimated. Consequently, 55% of model flooded areas are incorrect, and the model overestimates observed flood extent in 30%.

Flood extent errors of the model, mainly in low water period, are possibly due to uncertainty in some of model parameters such as river bottom level and width, vegetation height used to correct the DEM and also errors in the DEM. Large errors are found in Japurá floodplains, where water levels also present large errors in amplitude due to the underestimation of the cross-section width. Errors in low water period may also be due to the model assumption that the floodplain water level equals the water level at the main channel, since in reality, as river water levels fall, the connection between river and marginal lakes can be over, and the lakes will stop to empty. Other source of errors can be uncertainty in remote sensing flood extend estimates. According to Hess *et al.* (2003), user's accuracy at high water is 94% for the flooded class and 76% for the nonflooded class, while at low water, user's accuracy is 84% for flooded and 89% for nonflooded.

We also evaluated combined high and low water results. In this case, the model underestimated only 10% the total flooded area, only 20% of the predicted flood is incorrect and 29% of observed flood is missed by the model. Model accuracy ($TS = 0.60$) is comparable to other flood inundation modelling studies (e.g. Horritt and Bates, 2001; Horritt and Bates, 2002) and according to *BIAS*, model performance is similar or better than other modelling studies in the Amazon, e.g. Coe *et al.* (2008) overestimate in 30% the Hess *et al.* (2003) high water flood extent; Yamazaki *et al.* (2011) overestimate in 0.4% (3%) the Hess *et al.* (2003) high (low) water flood extent but greatly overestimates the multi-satellite observation flood extent by Prigent *et al.* (2007); while Decharme *et al.* (2011) greatly underestimates the multisatellite observation flood extent in the Amazon by Prigent *et al.* (2007).

Table III. Model performance statistics for water levels on the stream gauge stations

ID	Gauge	River	R	E_{NS}	A' (%)	A^{obs} (m)	DI [days]
20	12870000	(1) Auati-Paraná	**0.26**	**−0.21**	−24	9.52	**71**
23	13100000	(1) Coari	**0.79**	**0.24**	**54**	5.16	**29**
2	11444900	(1) Içá	**0.49**	**−0.57**	32	6.51	**−51**
21	12880000	(1) Tefé	**0.89**	0.74	8	5.35	**15**
	Mean		**0.61**	**0.05**	30	6.64	**42**
32	13650000	(2) Acre	**0.86**	**0.43**	**−70**	12.19	5
37	13840001	(2) Ituxi	0.93	**0.39**	**−75**	12.27	−1
38	13849000	(2) Ituxi	0.94	0.58	**−61**	12.73	−5
41	13885000	(2) Mucuim	0.94	0.83	−24	5.91	6
35	13740000	(2) Pauini	0.91	0.60	**−52**	10.84	1
42	13886000	(2) Tapaua	0.93	**0.27**	**84**	7.62	**16**
18	12845000	(2)Japurá	0.99	**−0.14**	**103**	7.69	1
19	12850000	(2)Japurá	0.92	**0.26**	**70**	6.53	8
	Mean		0.93	**0.40**	**67**	9.47	5
6	12230000	(3) Bia	**0.89**	0.79	−15	4.05	1
10	12520000	(3) Juruá	**0.89**	0.67	−36	10.56	−2
12	12550000	(3) Juruá	0.94	0.84	−17	13.08	2
16	12700000	(3) Juruá	0.94	0.79	−30	14.85	2
17	12840000	(3) Juruá	0.94	0.84	−14	13.17	4
4	12100000	(3) Jutaí	**0.89**	0.58	**−53**	8.37	0
5	12200000	(3) Jutaí	0.92	0.85	−5	6.26	−4
28	13410000	(3) Purus	**0.89**	0.79	−17	11.57	1
33	13700000	(3) Purus	0.94	0.80	−32	13.52	1
34	13710001	(3) Purus	0.94	0.81	−31	13.36	1
36	13750000	(3) Purus	0.95	0.84	−27	15.52	0
39	13870000	(3) Purus	0.97	0.88	−17	15.80	0
40	13880000	(3) Purus	0.96	0.90	−6	15.74	8
43	13955000	(3) Purus	0.94	0.88	−15	13.87	**15**
44	13962000	(3) Purus	0.95	0.90	−4	12.27	**14**
45	13980000	(3) Purus	0.96	0.92	−1	11.14	**10**
46	13990000	(3) Purus	0.97	0.95	−4	10.51	7
	Mean		0.93	0.83	19	11.98	4
1	11400000	(4) Solimões	0.99	0.98	−7	9.77	2
3	11500000	(4) Solimões	0.98	0.97	−4	10.00	2
7	12351000	(4) Solimões	0.98	0.97	0	9.86	1
22	12900001	(4) Solimões	0.97	0.91	−15	10.88	2
24	13150000	(4) Solimões	0.97	0.89	−23	10.52	4
47	14100000	(4) Solimões	0.98	0.95	−10	11.25	4
	Mean		0.98	0.95	10	10.38	3
	Mean		0.90	0.66	30	10.52	8
	90%		0.98	0.95	70	14.46	16
	50%		0.94	0.81	23	10.84	4
	10%		0.87	0.25	4	6.05	1

[a] Statistics computed from absolute values for A' and DI.
[b] Indexes marked in bold indicate the 25% worst values
[c] Stream gauge stations are grouped according to their location: (1) small tributaries of Solimões River; (2) tributaries of Purus River and Japurá River; (3) main Solimões tributaries, namely Purus, Juruá and Jutaí; and (4) Solimões River

Flood inundation versus backwater effects

In this section, we investigate the cause of the large differences between discharge results from HD and MC models. The main differences between basic model equations is that the HD considers (i) exchange (q_{fl}) and storage of water in floodplains and (ii) backwater effects trough the pressure term in the dynamic equation of the Saint Venant model. We discuss the importance of each of these factors on Amazon River hydraulics. Results of three model runs using different flow routing algorithms are analyzed: HD run - hydrodynamic model; MC run - Muskingum-Cunge model; HD' run - hydrodynamic model without exchange and storage of water on floodplains.

Table IV. Model performance statistics for flood extent: threat score (*TS*), missed flooded areas ratio (*MFR*), false alarm ratio (*FAR*) and bias index (*BIAS*)

Time period	*TS*	*MFR*	*FAR*	*BIAS*
High water	0.70	0.26	0.08	0.81
Low water	0.34	0.42	0.55	1.30
All	0.60	0.29	0.20	0.90

The simple comparison of hydrographs in large rivers of the three model runs (Figure 9) shows that the HD' results are very similar to the MC results, inducing one to conclude that flood waves are more affected by floodplain storage than by pressure term.

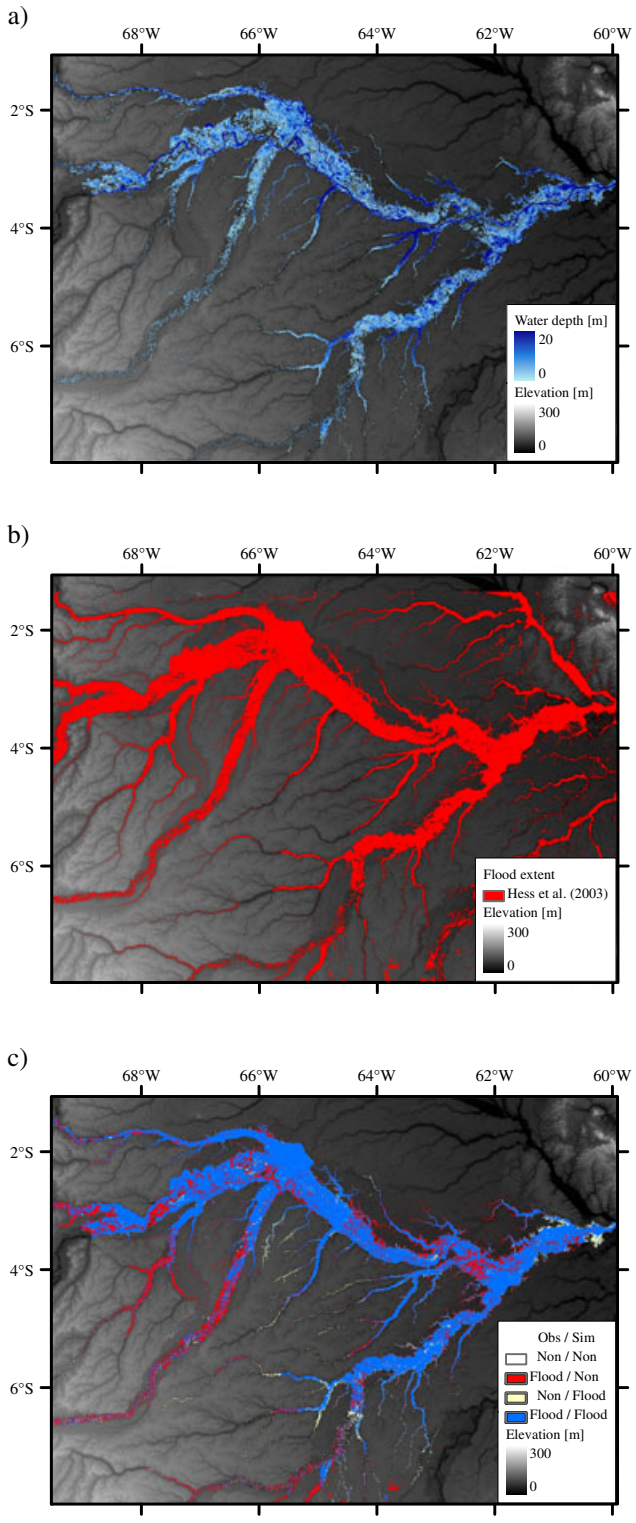

Figure 7. Solimões River flood inundation in high water period (May15-96): (a) simulated water depth, (b) flood extent estimates by Hess *et al.* (2003) and (c) error map

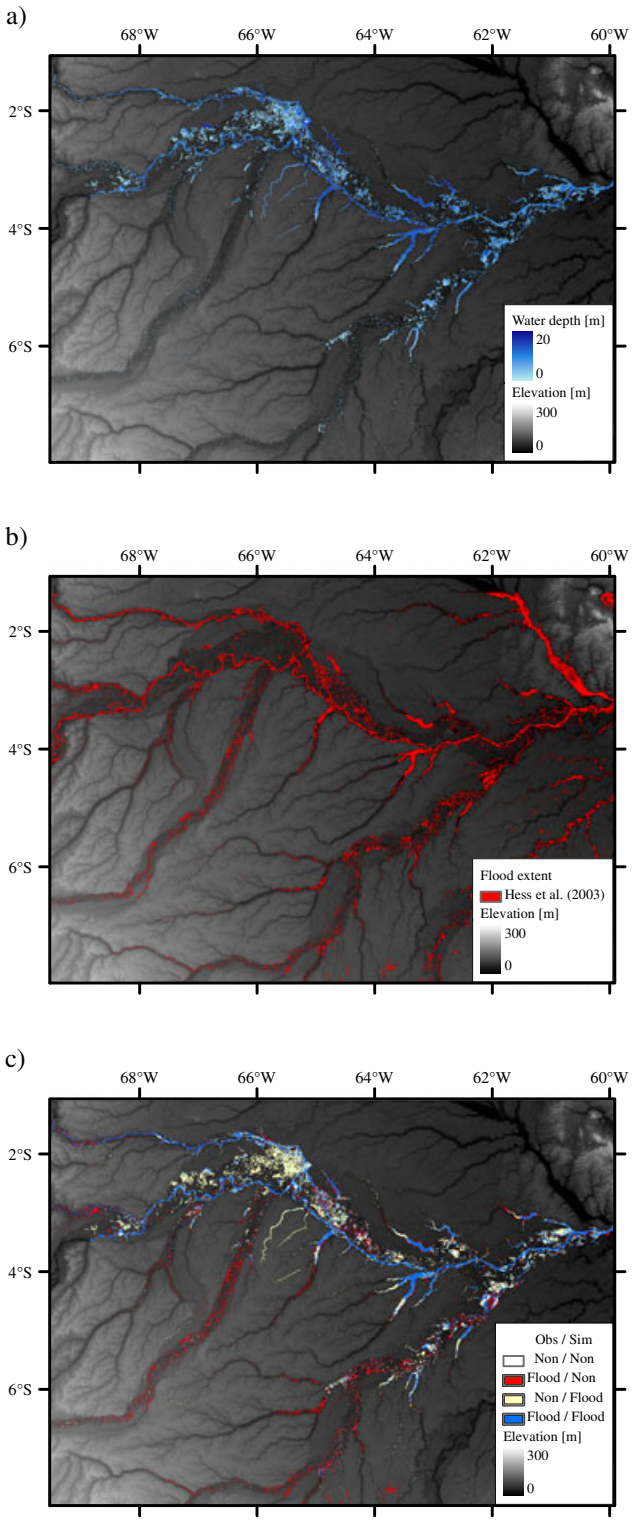

Figure 8. Solimões River flood inundation in low water period (Oct15-95): (a) simulated water levels, (b) flood extent estimates by Hess *et al.* (2003) and (c) error map

However, further analysis indicates that the pressure term plays an important role on floodplain storage. Figure 10 shows discharge and water level results of the HD and HD' runs in a small tributary of the Solimões River. Discharge in the HD run is much correlated to the water level derivative $\partial z/\partial t$ and not correlated to the water level. When the water level in Solimões River rises (falls), discharge on the tributary decrease (increase) and its floodplain store (release) water. This indicates that discharge is controlled by Solimões River backwater effects and not by its upstream catchment flood. Figure 10 also shows that when floodplain is not present, river discharge is correlated with water levels and controlled by upstream hydrology.

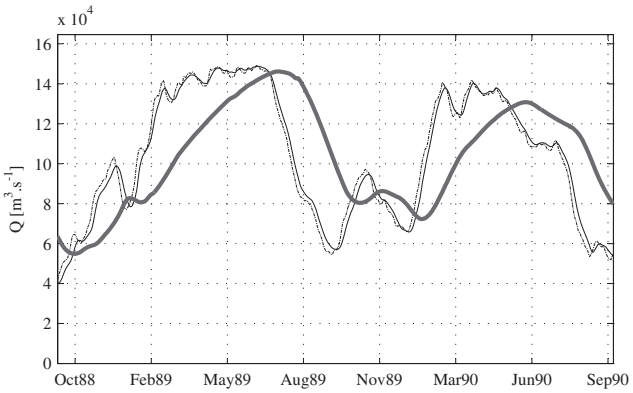

Figure 9. Simulated daily discharges in Manacapuru, close to the Solimões River outlet, from HD (bold grey line), HD' (thin black line) and MC (dashed line) model runs

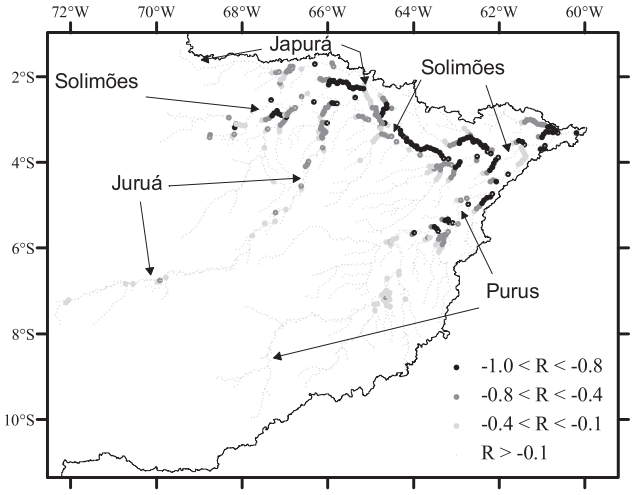

Figure 11. Correlation coefficient R between Q and $\partial z/\partial t$ on model computational cross sections

We calculated the correlation between Q and $\partial z/\partial t$ for each computational cross section to map this behavior (Figure 11). Negative correlations indicate that discharges are controlled by water levels of a downstream large river and backwater effects. Positive correlations do not indicate that backwater effects are not present, but that discharge is controlled mainly by upstream flood waves. Correlations on HD' runs (not shown here) are all positive and point that without the floodplains, backwater effects on discharge are less important. In contrast, correlations from HD run are negative in most tributaries of large rivers (Figure 11) and increase close to their confluences.

Yamazaki *et al.* (2011) performed similar experiments in the Amazon comparing a kinematic wave based without

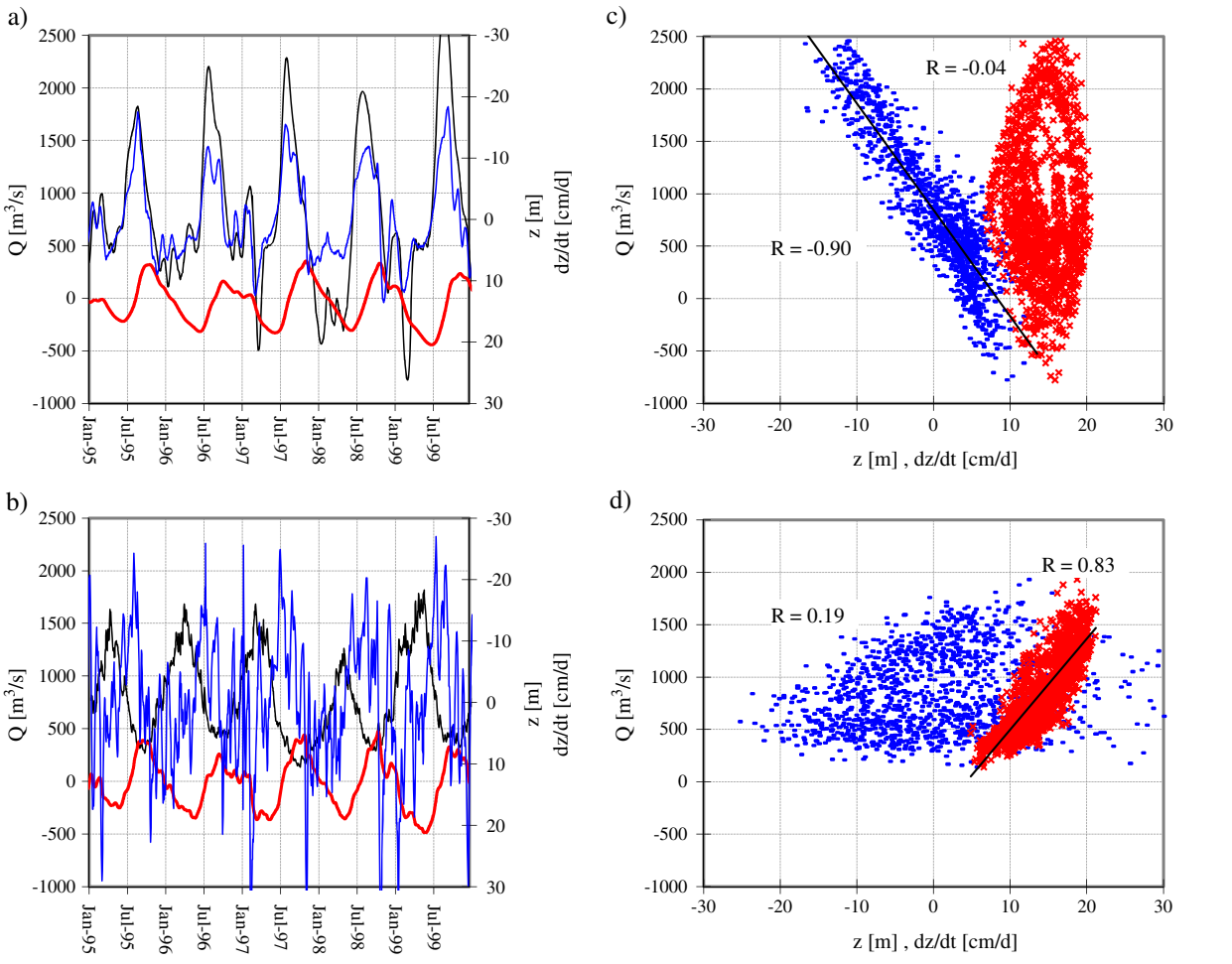

Figure 10. Discharge and water level relations in a small tributary of Solimões River. Simulated daily discharge (black line), water level (red dotted line) and water level derivative (blue line) from HD (a) and HD' (b) model runs. Simulated daily water level (red dots) and water level derivative (blue dots) *versus* discharge from HD (c) and HD' (d) model runs

floodplains (NoFLD), a kinematic wave (FLD + Kine) and a diffusion wave (FLD + Diff) with floodplains models, the latter considering the pressure term. Results in Óbidos show that, in accordance with our results, hydrographs from the NoFLD model are noisy and in advance. Hydrographs from FLD + Kine and FLD + Diff experiments fitted observations in Óbidos. However, hydrological regime from FLD + Kine and FLD + Diff is different in the major tributaries and is better represented when the pressure term is included. Besides, kinematic wave solution generated unrealistic water surface profiles, with negative slopes in some cases and the diffusive model provided better representation of flood extent.

The analyses show that both pressure term and backwater effects play an important role in floodplain storage and river discharge and are important in river hydrodynamics of the Solimões basin.

CONCLUSIONS

A model for large-scale hydrodynamic modelling developed in Paiva *et al*. (2011) was evaluated in the Solimões River basin. It is a limited data and GIS based large-scale hydrodynamic modelling approach, resultant from an improvement of the MGB-IPH model (Collischonn *et al*., 2007). The main differences of the large-scale HD against classical simplified flow routing algorithms are that it (i) represents backwater effects and floodplain storage; (ii) is full physic based; and (iii) provides additional output variables such as water level and 2 D flood inundations, in addition to discharge results.

Results show that the HD provides accurate discharge results and performs better than simplified flow routing algorithms represented by the MC model. Flood waves of Solimões River and its main tributaries are very attenuated and delayed, a behavior well represented by the HD model, contrasting with results from the MC approach, which provided hydrographs wrongly noisy and in advance.

The model is able to simulate the observed water levels with accuracy, representing their amplitude of variation and timing. Model accuracy is better in large rivers, and most of the errors concentrate in small rivers, possibly due to uncertainty in river geometry. Validation of the model flood extent results show that model performance is better in the high water period and some errors are found in the low water period. The overall model accuracy is comparable with other flood inundation modelling studies. Analyses suggest that the large-scale hydrodynamic modelling approach can be used for water levels and flood extent simulations.

We also investigate the cause of the large difference between the stream flow results of the HD and MC models. Results show that (i) river-floodplain water exchange and storage; and (ii) the pressure forces and backwater effects play an important role for the Amazon River hydrodynamics, namely the large travel times and the attenuation of its flood waves.

The proposed model uses a relatively complex and complete approach for river hydraulics modelling and a simplistic model for simulating floodplains. This model is aimed at providing discharge, water level and flood extent results at a large scale, by simulating translation and diffusion of flood waves, backwater effects and the influence of floodplain storage on flood waves. This floodplain modelling approach intents/tries to overcome the currently restrictions concerning computational resources and topography information of the floodplains, being oriented to large-scale applications and not for studying smaller scale floodplain hydraulics. Although having some restrictions, the model showed to be able to provide relatively accurate discharge, water level and flood extent results.

A full comparison of the performance of the model presented here with other recently developed models is difficult due to differences in forcing data and methods and data used in validation, etc. Still, we performed a detailed validation in terms of number of stream gauges, and performance showed to be similar or in some cases than other modelling studies in the Amazon. Moreover and more importantly, the analyses show that (i) backwater effects and floodplain processes play an important role for large-scale stream flow routing and inundation dynamics in the Amazon and possibly in other global large rivers and (ii) that a physic-based approach based on full Saint Venant equations may be feasible for large-scale applications, indicating that these features should be included in large-scale flow routing models.

ACKNOWLEDGEMENTS

The authors are grateful for: the financial and operational support from the Brazilian agencies FINEP and ANA as well as the constructive comments from Marie-Paule Bonnet, Daniel Allasia and Carlos E.M. Tucci, and also Dai Yamazaki and other two anonymous reviewers.

REFERENCES

Allasia DG, Collischonn W, Silva BC, Tucci CEM. 2006 Large basin simulation experience in South America. In: Predictions in Ungauged Basins: Promise and Progress. Proceedings of Symposium S7 held during the Seventh IAHS Scientific Assembly at Foz do Iguaçu, Brazil, April 2005. IAHS Publication 303, pp. 360–370.

Alsdorf D, Bates P, Melack J, Wilson M, Dunne T. 2007a. The spatial and temporal complexity of the Amazon flood measured from space. *Geophysical Research Letters* **34**: L08402.

Alsdorf D, Han S-C, Bates P, Melack J. 2010. Seasonal water storage on the Amazon floodplain measured from satellites. *Remote Sensing of Environment* **114**: 2448–2456.

Alsdorf DE, Rodriguez E, Lettenmaier DP. 2007b. Measuring surface water from space. *Reviews of Geophysics* **45**: RG2002. DOI: 10.1029/2006RG000197.

ANA. 2006. Topologia Hídrica: método de construção e modelagem da base hidrográfica para suporte à gestão de recursos hídricos. Versão 1.11. http://www.ana.gov.br.

Arora VK, Chiew FHS, Grayson RB. 1999. A river flow routing scheme for general circulation models. *Journal of Geophysical Research* **104**: 14,347–14,357, 1999.

Beighley RE, Eggert KG, Dunne T, He Y, Gummadi V, Verdin KL. 2009. Simulating hydrologic and hydraulic processes throughout the Amazon River Basin. *Hydrological Processes* **23**(8): 1221–1235.

Biancamaria S, Bates PD, Boone A, Mognard NM. 2009. Large-scale coupled hydrologic and hydraulic modelling of the Ob river in Siberia. *Journal of Hydrology* **379**: 136–150.

Bonnet MP, Barroux G, Martinez JM, Seyler F, Turcq PM, Cochonneau G, Melack JM, Boaventura G, Bourgoin LM, León JG, Roux E,

Calmant S, Kosuth P, Guyot JL, Seyler F. 2008. Floodplain hydrology in an Amazon floodplain lake (Lago Grande de Curuaí). *Journal of Hydrology* **349**: 18–30 pp.

Castellarin A, Di Baldassarre G, Bates PD, Brath A. 2009. Optimal Cross-Sectional Spacing in Preissmann Scheme 1D Hydrodynamic Models. *Journal of Hydraulic Engineering* **135**(2): 96–105.

Chow VT. 1959. *Open Channel Hydraulics*. McGraw-Hill: 680.

Coe MT, Costa MH, Howard EA. 2008. Simulating the surface waters of the Amazon River basin: Impacts of new river geomorphic and flow parameterizations. *Hydrological Processes* **22**(14): 2542–2553.

Collischonn W, Allasia DG, Silva BC, Tucci CEM. 2007. The MGB-IPH model for large-scale rainfall-runoff modeling. *Hydrological Sciences Journal* **52**: 878–895.

Collischonn B, Collischonn W, Tucci C. 2008. Daily hydrological modeling in the Amazon basin using TRMM rainfall estimates. *Journal of Hydrology* 207.

Collischonn W, Tucci CEM, Haas R, Andreolli I. 2005. Forecasting river Uruguay flow using rainfall forecasts from a regional weather-prediction model. *Journal of Hydrology* **305**: 87–98, 2005.

Cunge JA, Holly FM, Verney A. 1980. *Practical Aspects of Computational River Hydraulics*. Pitman Advanced Publishing Program.

Dadson SJ, Ashpole I, Harris P, Davies HN, Clark DB, Blyth E, Taylor CM. 2010. Wetland inundation dynamics in a model of land surface climate: Evaluation in the Niger inland delta region. *Journal of Geophysical Research* **115**: D23114. DOI: 10.1029/2010JD014474

Decharme B, Alkama R, Papa F, Faroux S, Douville H, Prigent C. 2011. Global off-line evaluation of the ISBA-TRIP flood model. *Climate Dynamics*, On line. DOI: 10.1007/s00382-011-1054-9)

Decharme B, Douville H, Prigent C, Papa F, Aires F. 2008. A new river flooding scheme for global climate applications: Off-line evaluation over South America. *Journal of Geophysical Research* **113**: D11110. DOI: 10.1029/2007JD009376

Dijkshoorn JA, Huting JRM, Tempel P. 2005. Update of the 1:5 million Soil and Terrain Database for Latin America and the Caribbean (SOTERLAC; version 2.0). Report 2005/01, ISRIC – World Soil Information, Wageningen.

Durand M, Fu LL, Lettenmaier D, Alsdorf DE, Rodríguez E, Fernandez DE. 2010. The surface water and ocean topography mission: Observing terrestrial surface water and oceanic submesoscale eddies. *Proceedings of the IEEE*. **98**(5): 766–779.

Eva HD, De Miranda EE, Di Bella CM, Gond V. 2002. *A Vegetation map of South America*. EUR 20159 EN, European Commission: Luxembourg.

Farr TG, Caro E, Crippen R, Duren R, Hensley S, Kobrick M, Paller M, Rodriguez E, Rosen P, Roth L, Seal D, Shaffer S, Shimada J, Umland J, Werner M, Burbank D, Oskin M, Alsdorf D. 2007. The shuttle radartopography mission. *Reviews of Geophysics* **45**(2).

Frappart F, Calmant S, Cauhopé M, Seyler F, Cazenave A. 2006. Preliminary results of ENVISAT RA-2-derived water levels validation over the Amazon basin. *Remote Sensing of Environment* **100**: 252–264.

Getirana ACV, Bonnet M-P, Rotunno Filho OC, Collischonn W, Guyot J-L, Seyler F, Mansur WJ. 2010. Hydrological modelling and water balance of the Negro River basin: evaluation based on in situ and spatial altimetry data. *Hydrological Processes* **24**(22): 3219–3236.

Hellweger F. 1997. AGREE - DEM Surface Reconditioning System. University of Texas, Austin, 1997. http://www.ce.utexas.edu/prof/maidment/GISHYDRO /ferdi/research/agree/agree.html.

Hess LL, Melack JM, Novo EMLM, Barbosa CCF, Gastil M. 2003. Dual-season mapping of wetland inundation and vegetation for the central Amazon basin. *Remote Sensing of Environment* **87**: 404–428.

Horritt MS, Bates PD. 2001. Effects of spatial resolution on a raster based model of flood flow. *Journal of Hydrology* **253**: 239–249.

Horritt MS, Bates PD. 2002. Evaluation of 1D and 2D numerical models for predicting river flood inundation. *Journal of Hydrology* **268**: 87–99.

Kalnay E, *et al*. 1996. The NCEP/NCAR 40-year Reanalysis Project. *Bulletin of the American Meteorological Society* **77**: 437–471.

Kosuth P, Callède J, Laraque A, Filizola N, Guyot JL, Seyler P, Fritsch JM, Guimarães V. 2009. Sea-tide effects on flows in the lower reaches of the Amazon River. *Hydrological Processes* **23**(22): 3141–3150.

Lehner B, Verdin K, Jarvis A. 2006. HydroSHEDS Technical Documentation. World Wiuldlife Fund US, Washington, DC. Disponível em http://hydrosheds.cr.usgs.gov

Lian Y, Chan I-C, Singh J, Demissie M, Knapp V, Xie H. 2007. Coupling of hydrologic and hydraulic models for the Illinois River Basin. *Journal of Hydrology* **344**: 210–222.

Liston GE, Sud YC, Wood EF. 1994. Evaluating GCM Land Surface Hydrology Parameterizations by Computing River Discharges Using a Runoff Routing Model: Application to the Mississippi Basin. *Journal of Applied Meteorology* **33**: 394–405.

Mauser W, Bach H. 2009. PROMET - Large scale distributed hydrological modelling to study the impact of climate change on the water flows of mountain watersheds. *Journal of Hydrology* **376**(3–4): 362–377.

Meade RH, Rayol JM, Da Conceição SC, Natividade JRG. 1991. Backwater effects in the Amazon River basin of Brazil. *Environmental Geology and Water Sciences* **18**(2): 105–114.

Nash JE, Sutcliffe JV. 1970. River flow forecasting through conceptual models, part I – a discussion of principles. *Journal of Hydrology* **10**: 282–290.

Nijssen B, Lettenmaier D. 2004. Effect of precipitation sampling error on simulated hydrological fluxes and states: Anticipating the Global Precipitation Measurement satellites. *Journal of Geophysical Research* **109**: D02103. DOI: 10.1029/2003JD003497

Paiva RCD. 2009. Large scale hydrological and hydrodynamic modeling: the Rio Solimões case study (in Portuguese). MSc dissertation, Instituto de Pesquisas Hidráulicas. Universidade Federal do Rio Grande do Sul. http://hdl.handle.net/10183/18927.

Paiva RCD, Collischonn W, Tucci CEM. 2011. Large scale hydrologic and hydrodynamic modeling using limited data and a GIS based approach. *Journal of Hydrology* **406**(3–4): 170–181.

Paz AR, Bravo JM, Allasia D, Collischonn W, Tucci CEM. 2010. Large-Scale Hydrodynamic Modeling of a Complex River Network and Floodplains. *Journal of Hydrologic Engineering* **15**(2): 152–165.

Perumal M, Sahoo B. 2008. Volume conservation controversy of the variable parameter Muskingum- Cunge method. *Journal of Hydraulic Engineering* **134**(4): 475–485.

Ponce VM. 1989. *Engineering Hydrology*. Prentice Hall.

Prigent C, Papa F, Aires F, Rossow WB, Matthews E. 2007. Global inundation dynamics inferred from multiple satellite observations, 1993–2000. *Journal of Geophysical Research* **112**: D12107. DOI: 10.1029/2006JD007847

RADAMBRASIL. 1982. Programa de Integração Nacional, Levantamento de Recursos Naturais. Ministério das Minas e Energia, Secretaria-Geral.

Remo JWF, Pinter N. 2007. Retro-modeling the Middle Mississippi River. *Journal of Hydrology* **337**: 421–435.

Singh VP, Frevert DK (eds). 2002. *Mathematical Models of Large Watershed Hydrology*. Water Resources Publications: Highlands Ranch, CO.

Sippel SJ, Hamilton SK, Melack JM, Novo EMM. 1998. Passive microwave observations of inundation area and the area/stage relation in the Amazon River floodplain. *International Journal of Remote Sensing* **19**(16): 3055–3074.

Tang X-N, Knight DW, Samuels PG. 1999. Volume conservation in variable parameter Muskingum-Cunge method. *Journal of Hydraulic Engineering* **125**(6): 610–620.

Todini E. 2007. A mass conservative and water storage consistent variable parameter Muskingum-Cunge approach. *Hydrology and Earth System Sciences* **11**: 1645–1659.

Tomasella J, Borma LS, Marengo JA, Rodriguez DA, Cuartas LA, Nobre CA, Prado MCR. 2010. The droughts of 1996–1997 and 2004–2005 in Amazonia: hydrological response in the river main-stem. *Hydrological Processes* **25**: 1228–1242.

Trigg MA, Wilson MD, Bates PD, Horritt MS, Alsdorf DE, Forsberg BR, Vega MC. 2009. Amazon flood wave hydraulics. *Journal of Hydrology* **374**: 92–105.

Tucci CEM. 1978. Hydraulic and Water Quality Model for a River Network. PhD dissertation, Colorado State University, Fort Collins, USA.

Vorosmarty CJ, Moore B, Grace AL, *et al*. 1989. Continental scale models of water balance and fluvial transport: an application to South America. *Global Biogeochemical Cycles* **3**(3): 241–265.

Wilks DS. 2006. *Statistical Methods in the Atmospheric Sciences*, (2d ed). International Geophysics Series **91**: Academic Press, pp. 627.

Wong THF, Laurenson EM. 1983. Wave Speed-Discharge Relations in Natural Channels. *Water Resources Research* **19**(3): 701–706.

Yamazaki D, Kanae S, Kim H, Oki T. 2011. A physically based description of floodplain inundation dynamics in a global river routing model. *Water Resources Research* **47**: W04501. DOI: 10.1029/2010WR009726

Yapo PO, Gupta HV, Sorooshian S. 1998. Multi-objective global optimization for hydrologic models. *Journal of Hydrology* **204**: 83–97.

